Published in final edited form as:

Cell Calcium. 2020 November ; 91: 102267. doi:10.1016/j.ceca.2020.102267.

Autonomous activation of CaMKII exacerbates diastolic calcium leak during beta-adrenergic stimulation in cardiomyocytes of Metabolic Syndrome rats

Tatiana Romero-García[1], **Huguet V Landa-Galván**[1], **Natalia Pavón**[2], **Martha Mercado-Morales**[1], **Héctor H Valdivia**[3], **Angélica Rueda**[1,*]

[1]Department of Biochemistry, Centro de Investigación y de Estudios Avanzados del IPN, Cinvestav-IPN, México City, 07300 México.

[2]Department of Pharmacology, Instituto Nacional de Cardiología “Ignacio Chávez”, México City, México.

[3]Department of Medicine, Division of Cardiovascular Medicine, University of Wisconsin School of Medicine and Public Health, Madison, WI, 53705, USA.

Abstract

Autonomous Ca^{2+}/calmodulin-dependent protein kinase II (CaMKII) activation induces abnormal diastolic Ca^{2+} leak, which leads to triggered arrhythmias in a wide range of cardiovascular diseases, including diabetic cardiomyopathy. In hyperglycemia, Ca^{2+} handling alterations can be aggravated under stress conditions via the β-adrenergic signaling pathway, which also involves CaMKII activation. However, little is known about intracellular Ca^{2+} handling disturbances under β-adrenergic stimulation in cardiomyocytes of the prediabetic metabolic syndrome (MetS) model with obesity, and the participation of CaMKII in these alterations.

MetS was induced in male Wistar rats by administering 30% sucrose in drinking water for 16 weeks. Fluo 3-loaded MetS cardiomyocytes exhibited augmented diastolic Ca^{2+} leak (in the form

[*]**Correspondence:** Angélica Rueda, Ph.D., Department of Biochemistry, Cinvestav-IPN, Av. IPN 2508. Col San Pedro Zacatenco, México City, 07360, México. Phone: +52 (55) 57473953, Fax: +52(55)57473951, arueda@cinvestav.mx.

Authors Contributions

Tatiana Romero-García: Conceptualization, Methodology, Investigation, Formal analysis, Visualization, Writing-original draft preparation. **Huguet V. Landa-Galván:** Conceptualization, Methodology. **Martha Mercado-Morales:** Methodology, Investigation; Natalia Pavón: ECG recordings and ECG analysis. **Héctor H. Valdivia:** Conceptualization, Resources, Writing-Review and Editing, Funding acquisition. **Angélica Rueda:** Conceptualization, Resources, Writing-Review and Editing, Project administration, Funding acquisition. All authors read and approved the final version of the manuscript.

Ethics approval and consent to participate

This study was carried out in accordance with the ethical guidelines of the Mexican Official Norm (NOM-062-ZOO-1999) and the National Institutes of Health Guide for the Care and Use of Laboratory Animals (NIH publication updated in 2011); it was also approved by the Institutional Bioethical Committee for Care and Handling of Laboratory Animals at the CINVESTAV-IPN (approved CICUAL Protocol No. 0105–14).

Competing interests

The authors declare that they have no competing interests.

Disclosures

None

of spontaneous Ca^{2+} waves) under basal conditions and that Ca^{2+} leakage was exacerbated by isoproterenol (ISO, 100 nM). At the molecular level, [^{3}H]-ryanodine binding and basal phosphorylation of cardiac ryanodine receptor (RyR2) at Ser2814, a CaMKII site, were increased in heart homogenates of MetS rats with no changes in RyR2 expression. These alterations were not further augmented by Isoproterenol. SERCA pump activity was augmented 48 % in MetS hearts before β-adrenergic stimuli, which is associated to augmented PLN phosphorylation at T17, a target of CaMKII. In MetS hearts. CaMKII auto-phosphorylation (T287) was increased by 80%. The augmented diastolic Ca^{2+} leak was prevented by CaMKII inhibition with AIP. In conclusion, CaMKII autonomous activation in cardiomyocytes of MetS rats with central obesity significantly contributes to abnormal diastolic Ca^{2+} leak, increasing the propensity for β-adrenergic receptor-driven lethal arrhythmias.

Graphical Abstract

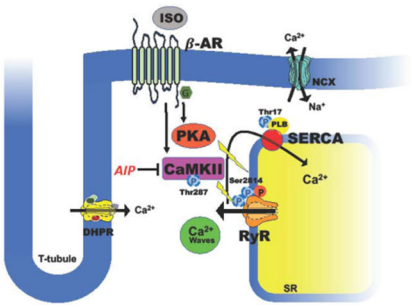

Keywords

Ca^{2+}/calmodulin-dependent protein kinase type II; diastolic Ca^{2+} leak; cardiac ryanodine receptor phosphorylation; β-adrenergic stimulation; metabolic syndrome; high sucrose diet

1. Introduction

Unhealthy contemporary lifestyles and dietary habits characterized by excessive consumption of carbohydrates and insufficient physical activity are associated with an alarming increase in the prevalence of obesity and cardiovascular diseases (CVDs) worldwide; the latter has become a global public health issue [1]. An early, adverse consequence of these unhealthy practices is the emergence of metabolic pathologies, which include Metabolic Syndrome (MetS). MetS represents a key risk factor for the development of Type II Diabetes Mellitus (DM2) and CVDs because the syndrome brings with it a series of such biochemical and physiological characteristics as obesity, high blood pressure, hypertriglyceridemia, low high-density lipoprotein cholesterol (HDL-c) levels, and insulin resistance with no alterations in fasting glucose levels [2–4]. The development of central obesity is considered an essential characteristic of MetS because it is an early step in the etiological cascade of the syndrome, linking waist circumference with CVD [5]. Thus, MetS is considered a pre-diabetic state and a key risk factor for heart disease [3]. Indeed, the prevalence of CVD events in subjects diagnosed with MetS is 31.9 %, but only 10.8 % in healthy subjects [6]. However, the molecular mechanisms underlying the higher incidence of

CVD events in MetS patients, either at resting or under stress conditions (for example, in the presence of β-adrenergic receptor stimulation), are not fully elucidated.

Disturbances in the activity of cardiac Ca^{2+} handling proteins have been reported in insulin resistance and diabetic cardiomyopathy—this is particularly true of proteins involved in excitation-contraction coupling (ECC) [7,8]. In the heart, ECC begins with Ca^{2+} influx via voltage-dependent L-type Ca^{2+} channels (VDCCs). This Ca^{2+} entry activates the intracellular Ca^{2+} channel/ryanodine receptor (RyR2) by Ca^{2+}-induced Ca^{2+} release, prompting a transient increase in the intracellular Ca^{2+} concentration ($[Ca^{2+}]_i$), which is followed by cell contraction. Relaxation takes place due to a Ca^{2+} clearance process that primarily involves (1) Ca^{2+} recapture into the sarcoplasmic reticulum (SR) Ca^{2+} stores through the action of the SR Ca^{2+} ATPase (SERCA pump) and (2) Ca^{2+} extrusion through the sarcolemmal Na^+/Ca^{2+} exchanger (NCX) [9]. The β-adrenergic response, induced by stress or strenuous physical activity, is the main regulatory pathway of the ECC mechanism [10,11]. Consequently, several ECC proteins—including VDCCs, RyRs, and phospholamban (PLN)—are phosphorylated by cAMP-dependent protein kinase (PKA), and Ca^{2+}/calmodulin-dependent kinase type II (CaMKII), which increases their activity.

CaMKII has been proposed as a key kinase contributing to the deleterious effects of chronic β-adrenergic receptor activation in cardiac pathologies, mainly by exacerbating RyR2-mediated diastolic Ca^{2+} leak [12,13]. Studies in experimental models of insulin resistance and fructose fed-induced pre-diabetic cardiomyopathy have unveiled the participation of hyperglycemia and ROS in inducing abnormal CaMKII activation, the latter has been associated with alterations in cardiomyocyte Ca^{2+} handling and with the appearance of cardiac arrhythmic events [14–16]. Hyperglycemia leads to CaMKII glycosylation, increasing RyR2-mediated Ca^{2+} leak, and reducing SR Ca^{2+} load in cardiac cells [14]. The duration of CaMKII activation relies on the frequency of Ca^{2+} release events. Prolongation of CaMKII activation is related to auto-phosphorylation of the kinase at T287: this prevents CaMKII auto-inhibition, which causes the kinase to remain active even when $[Ca^{2+}]_i$ declines, constituting a mechanism for CaMKII autonomous activation [13,17].

Remarkably, the role of CaMKII in Ca^{2+} handling alterations of non-hyperglycemic prediabetic cardiomyocytes from an experimental model of MetS with obesity and under β-adrenergic stress has not been previously studied. Therefore, we investigated (1) the effects of β-adrenergic-mediated CaMKII activation in Ca^{2+} handling alterations of MetS cardiomyocytes and (2) the underlying CaMKII-related molecular mechanisms.

2. Materials and methods

2.1. Sucrose-induced Metabolic Syndrome model

Recently weaned male *Wistar* rats were divided into two groups and maintained in sterile conditions with a 12 h dark-light cycle of 12 h and controlled temperature of 22 ± 2 °C. The control group (CTL) received plain water, while the Metabolic Syndrome group (MetS) received 30% sucrose (refined commercial sugar) via drinking water; both groups were fed with commercial rat chow ad libitum (PicoLab Rodent Diet 20, LabDiet St. Louis, MO, USA). The animals were used for experimentation after 16 weeks of treatment.

2.2. Measurement of body and serum parameters

After fasting overnight, the rats were treated with 1000 U/kg heparin (Pisa, Guadalajara, México) and anesthetized with sodium pentobarbital (Pisa, Guadalajara, México), as previously described [18]. Measurements of serum glucose, triglycerides (TG), and HDL-Cholesterol (HDL-C) were obtained from whole blood samples using glucose and lipid panel strips (PTS lipid panel and PTS glucose strips) with the CardioCheck PA analyzer (PTS Diagnostics, Indianapolis, IN, USA). Other parameters such as body weight, tibia length, heart weight, left ventricle weight, visceral fat weight, and blood pressure were also determined.

2.3. Ventricular myocyte isolation

Rat ventricular myocytes were obtained using a previously reported enzymatic perfusion method [19]. Briefly, hearts were rapidly excised from anesthetized animals and placed in ice-cold, oxygenated Tyrode solution containing (in mM: NaCl 130, KCl 5.4, $MgCl_2$ 0.5, NaH_2PO_4 0.4, glucose 22, HEPES 25; pH 7.4 with NaOH). Aortas were cannulated above the aortic valve and perfused with Tyrode solution supplemented with 0.23 mM EGTA for 5 min at 37 °C. Enzyme solution containing 1 mg/mL of collagenase Type II (Worthington Biochemical Corporation, Lakewood, NJ, USA) in Tyrode solution supplemented with 0.1 mM $CaCl_2$ was perfused until aortic valves were digested, as exhibited by increased efflux of perfusate. Hearts were then transferred to a tube containing enzyme solution supplemented with 10 mg/mL of BSA and gently shaken for 3 min at 37 °C to disperse myocytes. The resulting cell suspension was centrifuged for 3 min at 170 × *g*. The cell sedimentation was repeated two times, while $CaCl_2$ concentration on Tyrode solution was gradually increased (in mM: 0.25 and 0.5). Finally, the cell pellet was suspended in storage Tyrode solution supplemented with 0.8 mM $CaCl_2$.

2.4. Confocal Ca^{2+} Imaging

Isolated ventricular myocytes were loaded with the fluorescent Ca^{2+} indicator Fluo-3 AM (final concentration, 5 μM. Thermo Scientific Inc., Waltham, MA USA) for 25 min at room temperature. Fluo 3-loaded cardiomyocytes were placed in a field stimulation chamber with platinum electrodes (Warner Instruments LLC, Hamden CT, USA) attached to a perfusion system with valve controller (Model VC-6M, Warner Instruments LLC, Hamden CT, USA) and filled with recording Tyrode solution (in mM: NaCl 130, $CaCl_2$ 1, $MgCl_2$ 2.0, KCl 5.4, glucose 11, HEPES 10, pH 7.4 with NaOH). To activate the β-adrenergic response, Isoproterenol (ISO) was added to the recording Tyrode solution (final concentration 100 nM). Autocamptide-2 related inhibitory peptide (AIP, Cat N. SCP0001, Sigma Aldrich) was used in its myristoylated form for better membrane permeability. Cells were preincubated with AIP (10 μM, 1 h) in storage Tyrode solution before Ca^{2+} signaling recordings. Ca^{2+} sparks and Ca^{2+} waves were recorded in quiescent cardiomyocytes using a confocal microscope (Zeiss LSM700, Carl Zeiss Microscopy GmbH, Jena, Germany) in line-scan mode (1.5 ms/line). For this procedure, Fluo 3-loaded cardiomyocytes were paced at 0.5 Hz, electrical stimulation was stopped and confocal recordings (10 images per cell) were performed in quiescent cells after 5 min, in a lapse time of 20 min before washing the recording chamber and adding new Fluo 3-loaded cells. Ca^{2+} spark and Ca^{2+} wave

frequencies were calculated as the ratio of the total number of events per cell divided by the recording time (events/s). Parameters such as amplitude (F/F_0), full width at half maximum (FWHM, in μm), full duration at half maximum (FDHM, in ms), time-to-peak (ms), and decay time constant (in ms) were measured using IDL version 5.5 software (Research Systems Inc., Boulder CO, USA) for image analysis, running a specialized home-made protocol written by Ana Maria Gómez (Inserm UMR-S 1180, LabEx LERMIT, Châtenay-Malabry, France). Ca^{2+} spark-mediated Ca^{2+} leak was calculated by multiplying spark frequency*amplitude*duration*width (as described by Biesmans et al. [20]). To determine SR Ca^{2+} load, cells were paced for at least 5 min at 0.5 Hz using an electric field stimulator (set a 70 V with a pulse duration of 20 ms) to restore steady-state SR Ca^{2+} load, after which a 10 mM caffeine stimulus was applied through a perfusion system with valve controller (Model VC-6M, Warner Instruments LLC, Hamden CT, USA). The confocal images were analyzed using Origin 8.1 software (Origin Lab Corporation, Northampton MA, USA) and SR Ca^{2+} load was measured by the amplitude of the caffeine-evoked Ca^{2+} transient.

2.5. Determination of basal $[Ca^{2+}]_i$

Diastolic $[Ca^{2+}]$ was determined using an inverted microscope (Nikon Diaphot) coupled to a PTI microfluorometry system (RatioMaster™, PTI Technologies Inc. Oxnard CA, USA). Isolated ventricular cardiomyocytes were incubated with Fura-2 AM for 25 min at room temperature and washed. Fura 2-loaded cells were placed in a field stimulation chamber with platinum electrodes; the chamber was filled with recording Tyrode solution supplemented with $CaCl_2$ 1.8 mM. The cardiomyocytes were electrically stimulated at a frequency of 0.5 Hz before Fura-2 fluorescence signal was recorded. Diastolic $[Ca^{2+}]$i was calculated using the Grynkiewicz equation [21]. The values of Rmax (7.01) and Rmin (0.22) were obtained in the presence of 2.5 mM of Ca^{2+} and 2 mM of EGTA, respectively; the Kd used was 282 nM.

2.6. Preparation of left ventricle homogenates

Left ventricle homogenates were prepared as previously described [18] with some modifications. Excised rat hearts were placed in ice-cold Tyrode solution. Aortas were cannulated, and hearts were placed in a Langendorff perfusion system. Hearts were retroperfused with warm (37 °C) oxygenated Tyrode solution supplemented with EGTA 0.23 mM for 5 min to stop beating and clean the remaining blood. Hearts were then retroperfused with Tyrode solution containing $CaCl_2$ 1.8 mM to restore extracellular Ca^{2+} levels. The β-adrenergic response was stimulated with ISO 1 μM for an additional 5 min. At the end of the perfusion protocol, left ventricles (LV) were isolated and frozen in liquid N_2 before pulverization. The tissue powder was homogenized in a Potter-Elvehjem glass homogenizer at 400 rpm for 45 s with lysis buffer (in mM: HEPES 20 and sucrose 0.3, pH 7.2. with KOH) supplemented with protein inhibitors: leupeptin 12 μM, PMSF 100 μM, benzamidine 500 μM, and aprotinin 0.153 μM, and with phosphatase cocktail inhibitor 3 (MilliporeSigma Corp. St. Louis MO, USA). LV homogenates were centrifuged at 2000 *g* for 10 min, and supernatants aliquoted and frozen at −80°C. Protein concentrations were determined using the Lowry method.

2.7. [^{3}H]-ryanodine binding assay

To determine the maximum number of active RyRs, [^{3}H]-ryanodine binding assays were performed using LV homogenates as previously reported [19,22], with some modifications. Briefly, 50 μg of protein per tube were incubated with 7 nM [^{3}H]-ryanodine (PerkinElmer, Waltham MA, USA) for 90 min at 37°C in an incubation medium containing (in mM): 200 KCl, 20 HEPES (pH 7.2 with KOH), and $CaCl_2$ necessary to set free Ca^{2+} at 10 μM, as calculated by MaxChelator (http://maxchelator.stanford.edu/index.html). The samples were filtered onto glass fiber filters (Whatman GF-B, GE Healthcare, Chicago IL, USA) and washed three times with distilled water in an automatic collector (Brandel M24-R). The filters were placed in scintillation vials with 5 mL of liquid scintillation mixture, and the retained radioactivity was measured in a Beckman LS-6500 counter. The specific [^{3}H]-ryanodine binding was defined as the difference between the binding in the absence (total binding) and the presence (nonspecific binding) of 20 μM unlabeled ryanodine (MP Biomedicals LLC, Santa Ana CA, USA).

2.8. ATPase activity assay

Inorganic phosphate (Pi) production due to ATP cleavage by thapsigargin-sensitive ATPases was determined as previously described [19], following the protocol reported by Bartolommei et al., [23] with some modifications. LV homogenates (100 μg of protein per tube) were incubated in buffer solution with ~10 μM free [Ca^{2+}] (in mM: KCl 80, $MgCl_2$ 3, $CaCl_2$ 0.2, sodium azide 5, K-EGTA 0.2, MOPS 25, and A23187 0.002 at pH 7.0 adjusted with TRIS) at 37 °C for 5 min. The enzymatic reaction was initiated by adding 1mM ATP. Aliquots of 0.1 ml were taken after 5, 10, 15 and 30 min and were immediately added to 0.9 ml of Pi coloring solution (in mM: H_2SO_4 125, ascorbic acid 10, ammonium-heptamolybdate tetrahydrate 0.5 and potassium antimony (III) tartrate hydrate 0.04). Absorbance was measured after 10 min at 850 nm (Beckman Spectrophotometer DU800). Control experiments were performed in the presence of 100 nM thapsigargin. The difference between total and thapsigargin-insensitive ATPase activities was considered SERCA pump hydrolytic activity.

2.9. SDS-PAGE and Western Blots

Gradient polyacrylamide gels (4–12%) were loaded with the indicated amount of protein from LV homogenates in Laemmli buffer. The SDS-PAGE resolved proteins were transferred to PVDF membranes that were subsequently blocked for 1 h at room temperature with low fat dry milk 5% in PBS-T or TBS-T buffer when indicated; PVDF membranes were then incubated with corresponding primary antibodies against: RyR2 (ab2827, Abcam, Cambridge MA, USA), pS2808-RyR2 (A010–30, Badrilla, Leeds UK), pS2814-RyR2 (A010–31, Badrilla, Leeds UK), SERCA2 (ab2861, Abcam, Cambridge MA, USA), PLN (A010–14, Badrilla, Leeds UK), pS16-PLN (A010–12, Badrilla, Leeds UK), pT17-PLN (A010–13, Badrilla Leeds UK), CaMKII (4436s, Cell Signaling, Danvers MA, USA), pT287-CaMKII (12716s, Cell Signaling. Danvers MA, USA); and GAPDH (Cat# AM4300, Ambion®, Thermo Fisher Scientific, Waltham, MA, USA) for 2 h at room temperature. After washing, the PVDF membranes were incubated with corresponding secondary conjugated-HRP antibody (goat anti-mouse IgG Cat. # 401215 and goat anti-rabbit IgG Cat.

401315, MilliporeSigma Corp. St. Louis MO, USA) for 1 h at room temperature. Proteins were visualized by chemiluminescent reaction (SuperSignal® West Pico Chemiluminescent Substrate, Thermo Fisher Scientific, Waltham MA, USA) and the relative amount of protein was determined by densitometric analysis using ImageJ software (v. 1.50i NIH, USA).

2.10. AIP treatment of cardiomyocytes

Isolated ventricular myocytes were plated in 6-well plates with 1 mL of Tyrode solution supplemented with $CaCl_2$ 1 mM. After 10 min at 37 °C, cells were treated with AIP 10 μM for 1 h at 37 °C. The β-adrenergic response was induced with ISO 100 nM for an additional time of 10 min. At the end of the stimulation protocol, cells were collected and transferred to Eppendorf tubes and centrifuged at 3,000 rpm for 1 min. The supernatants were discarded, and pellets were immediately frozen in liquid N_2 and stored at −80 °C until use.

Cell pellets were resuspended in 100 μL of Laemmli buffer 1X, vortexed and sonicated for 40 s at 40 kHz. Then, the samples were heated at 99 °C for 5 min and centrifuged at 14,500 rpm for 5 min, supernatants were aliquoted and stored at −20 °C for future use in Western Blots. Protein was quantified using the RC-DC protein assay kit (BioRad) following the manufacturer's instructions.

2.11. Statistical data analysis

Data are presented as the mean ± standard error of the mean (M ± S.E.M). The number of animals for each experiment is designated by "N", while the number of cells or independent experiments is indicated as "n". The Shapiro-Wilk normality distribution test was used to determine the Gaussian distribution of the values. When sets of data failed normality distribution test, non-parametric tests were used to evaluate statistical significance, either Mann-Whitney rank sum test or Kruskal-Wallis One-Way ANOVA on ranks followed by Dunn's post-hoc test when appropriate. For sets of data with a normal Gaussian distribution, statistical significance was evaluated by two-tailed Student's *t*-test or One-Way ANOVA followed by Tukey post-hoc test when appropriate. A P value of ≤ 0.05 was considered statistically significant. All analyses were performed using Origin Pro v.8 software (Origin Lab Corporation, Northampton MA, USA) or Sigma Plot v11.0 (Systat Software Inc., San Jose, CA, USA).

3. Results

3.1 Characteristics of Metabolic Syndrome rats

Administration of 30 % sucrose in the drinking water of male *Wistar* rats for 16 weeks caused many common features of prediabetic Metabolic Syndrome, including a significant rise in body weight (32 %) and a 3.1-fold increase in abdominal fat accumulation compared to the control group (Table 1). Although the heart-weight-to-body-weight ratio was decreased in MetS rats, features such as left ventricle weight and left ventricle-to-heart weight ratio of the rats showed no alterations, ruling out any cardiac remodeling produced by the sucrose diet (Table 1). In MetS rats, dyslipidemia was evidenced by a 2-fold increase in total triglyceride levels and a reduction in HDL-cholesterol levels (15 %), with no alteration in serum fasting glucose levels compared with control animals (Table 1). There

was a 3.4-fold increase in the TG-to-HDL-C ratio in MetS rats, which is indicative of higher cardiometabolic risk in the insulin-resistant condition.[24].

3.2 Abnormal diastolic Ca^{2+} leak in MetS cardiomyocytes is exacerbated after β-adrenergic stimulation

The primary outcomes of cardiometabolic risk in MetS patients are myocardial infarction, coronary and peripheral arterial diseases, congestive heart failure, arrhythmia, and stroke [7]. Previous studies have documented a direct association between abnormal diastolic Ca^{2+} leak in cardiomyocytes and Ca^{2+}-driven cardiac arrhythmias [22,25]. The evidence of lethal arrhythmogenic activity in MetS rats (Supplementary Figure 1), also previously showed in sucrose-fed animals [26–28], prompted us to examine whether intracellular Ca^{2+} dynamics were compromised in this metabolic condition. A method for studying potential alterations of RyR2 activity in situ is by analyzing diastolic Ca^{2+} release events, such as spontaneous Ca^{2+} sparks and Ca^{2+} waves. Figures 1A and 1B show representative bi-dimensional images of these Ca^{2+} release events recorded with a confocal microscope in isolated Fluo 3-loaded cardiomyocytes. Recordings were taken under quiescent conditions and in the presence (or in the absence) of the β-adrenergic receptor agonist, isoproterenol (ISO). Under basal conditions (no ISO added), Ca^{2+} wave frequency was significantly higher in MetS cells compared with CTL cells (Figure 1C and Figure 1D), evidencing abnormal diastolic Ca^{2+} leak in the form of spontaneous Ca^{2+} waves in MetS cardiomyocytes.

As expected, ISO treatment increased Ca^{2+} spark frequency in cardiomyocytes of both experimental groups. Interestingly, the augmentation in Ca^{2+} spark frequency was larger in MetS cardiomyocytes (34 %) than in the CTL cells (20 %) (Figure 1C). However, ISO treatment significantly increased the Ca^{2+} spark-mediated Ca^{2+} leak (38 % respect to basal condition) in MetS cells only (Table 2). It is important to note that the Ca^{2+} spark amplitude remained unchanged in all the conditions, however, Ca^{2+} spark duration and width are decreased in MetS cell with and without ISO (Table 2). Histogram distributions of Ca^{2+} spark properties showed that the proportion of events with reduced duration and size is augmented in MetS cells may be due to the propensity of RyR clusters to be recruited to generate Ca^{2+} waves (Supplementary Figure 2 and Supplementary Table 1). Further analysis showed that β-adrenergic stimulus exacerbates already abnormal Ca^{2+} release in the form of spontaneous Ca^{2+} waves in MetS cardiomyocytes (Figure 1D), which attenuate changes in Ca^{2+} sparks properties (Supplementary Table 1). For cardiomyocytes of CTL group, we found that these modifications in diastolic Ca^{2+} dynamics are related to a significant increase in the SR Ca^{2+} load. The SR Ca^{2+} load was not modified in the MetS condition (Figure 1E, Supplementary Figure 3). Basal [Ca^{2+}] did not change in any of the experimental groups (Figure 1F). These data suggest that in MetS cardiomyocytes, mainly Ca^{2+} wave-mediated Ca^{2+} leak under basal conditions could be exacerbated by the β-adrenergic stimulus and may underlie cardiac arrhythmogenic activity.

3.3 Increased basal activity of RyR2s in MetS hearts is not further augmented by the β-adrenergic stimulus.

A possible explanation for the elevated incidence of diastolic Ca^{2+} release events in the MetS cardiomyocytes despite a similar SR Ca^{2+} load is the fact that activating the β-

adrenergic signaling pathway increases RyR2 activity in situ [29]. To explore this possibility, we performed [^{3}H]ryanodine binding assays in heart homogenates of MetS and CTL rats. Our results showed that under basal conditions (no ISO added) the maximum amount of active RyR2 at optimal [Ca^{2+}] (5 μM) was higher (47 %) in MetS preparations with respect to controls; this was not further increased by ISO treatment (Figure 2A). These results suggest that the abnormal Ca^{2+} leak in MetS may be due to exacerbated basal activity of RyR2s. Next, we explored the molecular mechanisms underlying these changes. Because increases in the expression level or the phosphorylation status of RyR2s may account for the augmentation in RyR2 activity [30], we measured total RyR2 protein expression and RyR2 phosphorylation status by Western Blot. Figure 2B shows representative immunoblots of phosphorylated and total RyR2s from heart homogenates, both untreated and treated with ISO. There was no significant difference in the total amount of RyR2s under all experimental conditions (Figure 2C); this effectively rules out alterations in the expression of RyR2 as an explanation for the augmented basal RyR2 activity observed in MetS hearts.

Conversely, the state of RyR2 phosphorylation at different residues can modify its activity [29]; therefore, we evaluated the phosphorylation levels of S2808 and S2814, two RyR2 sites identified as targets of PKA/CaMKII and CaMKII kinases, respectively. Basal phosphorylation levels of S2808 were substantially elevated—even in the absence of β-adrenergic stimulus; regardless, ISO treatment increased this parameter only for the CTL group (Figure 2D). Our data agree with previous work reporting that the phosphosite S2808 is at least ~50% constitutively phosphorylated [29,31]. Notably, MetS heart preparations under resting conditions had 59 % higher phosphorylation of S2814 than CTL heart homogenates; this augmented phosphorylation was not further increased by ISO treatment (Figure 2E).

3.4 Increased SERCA pump activity in MetS hearts under resting conditions compensates for augmented diastolic Ca^{2+} leak.

The abnormal diastolic Ca^{2+} leak observed in MetS cardiomyocytes under resting conditions may be associated with augmented basal RyR2 activity. However, caffeine-induced Ca^{2+} transients showed that SR Ca^{2+} load was not modified in MetS cardiomyocytes; this observation prompted us to evaluate whether perturbation of the SR Ca^{2+} recapture mechanism could explain the increase in Ca^{2+} availability for RyR2 release. The assessment of SERCA pump hydrolytic activity revealed that its Ca^{2+} recapture function was significantly increased in the hearts of MetS rats under basal conditions; this was not further increased with the β-adrenergic challenge. Conversely, ISO treatment did increase ATPase hydrolytic activity in CTL preparations (Figure 3A and 3B). The abnormal SERCA pump ATPase activity observed in MetS heart preparations was not due to changes in SERCA2 pump expression (Figure 3C and 3D).

3.5 CaMKII-induced phospholamban phosphorylation underlies augmented SERCA pump activity in MetS

Considering that phospholamban (PLN) is the main regulatory protein of SERCA pump activity [32], we determined the total protein expression levels of PLN. We also investigated PLN phosphorylation status at two different sites: S16 and T17, PKA-dependent and

CaMKII-dependent phosphorylation sites, respectively. Figure 4A shows representative PLN immunoblots of phosphorylated and total PLN from heart homogenates, treated (or not) with ISO. Our results show that under resting conditions, PLN was not phosphorylated at S16 in either experimental group; activation of the β-adrenergic response significantly increased S16-PLN phosphorylation (Figure 4B). Notably, T17 site was found to be phosphorylated under basal conditions in MetS heart preparations; further, β-adrenergic stimulus significantly increased T17-PLN phosphorylation only in CTL preparations (Figure 4C). Total PLN expression and PLN/SERCA pump ratio were similar for both experimental groups (PLN/SERCA pump, normalized data: 1.0 ± 0.13 in n = 5 control samples *vs.* 0.80 ± 0.13 in n=5 MetS heart preparations, $P < 0.3154$).

3.6 CaMKII is constitutively active in MetS hearts

The phosphorylation pattern of S2814-RyR2 and T17-PLN provided important insight into the participation of CaMKII in these post-translational modifications [33]; thus, we determined CaMKII expression and CaMKII auto-phosphorylation levels at the T287 site using Western Blot analysis (Figure 5). We primarily evaluated this post-translational modification because of its participation in the autonomous activation mechanism of CaMKII [13]. Figure 5A shows representative CaMKII immunoblots of pT287-CaMKII and total CaMKII from heart homogenates, untreated or treated with ISO. Our results demonstrate that under basal conditions, CaMKII auto-phosphorylation levels were significantly augmented (80%) in MetS heart homogenates compared to CTL samples (Figure 5C). ISO treatment did not increase the phosphorylation of T287 in CaMKII in either experimental group (Figure 5C). Moreover, CaMKII protein expression levels were unchanged in MetS homogenates (Figure 5B). Thus, CaMKII is constitutively active in MetS hearts: this autonomous activation may play a key role in the abnormal activity of RyR2s and SERCA pump under resting conditions.

3.7 CaMKII inhibitor AIP reduces diastolic Ca^{2+} leak in MetS cardiomyocytes

Although the augmented auto-phosphorylation levels of T287-CaMKII suggested a role for CaMKII in the abnormal diastolic Ca^{2+} leak observed in MetS cardiomyocytes, further evidence was required. To better understand CaMKII role in cardiovascular pathologies, KN-93 has been used as its inhibitor of choice; however, this methoxy-benzene-sulfonamide mainly blocks Ca-CaM-mediated CaMKII activation not its autonomous activation [34]. Thus, we used autocamptide-2-related inhibitory peptide (AIP) to inhibit CaMKII. We measured properties of Ca^{2+} sparks and Ca^{2+} waves in cardiomyocytes pre-incubated with AIP (10 μM, 1 h) (Figure 6A and 6B). In the presence of AIP, Ca^{2+} spark frequency augmented in the presence of the β-adrenergic stimulus (Figure 6C). Importantly, the abnormal diastolic Ca^{2+} leak in the form of Ca^{2+} waves in MetS cardiomyocytes, observed before and after the β-adrenergic stimulus, was now prevented.

Interestingly, although pre-incubation with AIP increased Ca^{2+} wave frequency in the CTL group, it inhibited the Ca^{2+} wave release in MetS cardiomyocytes (Figure 6D); further, preincubation with AIP prevented the increase in Ca^{2+} waves previously observed after β-adrenergic stimulus (Figure 1D).

In addition, Ca^{2+} spark amplitude and Ca^{2+} spark size were significantly diminished while Ca^{2+} spark time-to-peak was augmented by AIP in MetS cells, either treated or not with ISO (Table 3); suggesting a reduction of RyR2 activity. Thus, AIP treatment significantly decreased the Ca^{2+} spark-mediated Ca^{2+} leak in MetS cells regardless of ISO challenge. Histogram distributions of Ca^{2+} spark properties in AIP-treated cells (Supplementary Figure 4 and Supplementary Table 2) showed that the proportion of events with reduced amplitude and size is augmented in MetS cells. The AIP effect on the aforementioned Ca^{2+} spark properties remained even with ISO challenge; thus, the outcome was a significant decrease in Ca^{2+} spark-mediated Ca^{2+} leak. Additional Ca^{2+} spark properties were unaffected in MetS cells after exposure to AIP (Table 3). It is important to note that the differences observed in Ca^{2+} spark and Ca^{2+} wave incidence before and after ISO treatment were not associated with disturbances in SR-Ca^{2+} load or basal fluorescence (Figure 6E and 6F). The inhibition of abnormal diastolic Ca^{2+} leak in AIP-treated MetS cardiomyocytes is consistent with a significant reduction of RyR S2814 phosphorylation by CaMKII inhibition (Supplementary Figure 5) respect to basal MetS condition (pRyR S2814/RyR2 normalized data: 0.77 ± 0.12 in N = 5 AIP-treated cardiomyocyte samples *vs.* 1.66 ± 0.26 in N = 5 MetS heart preparations; $P = 0.036$).

4. Discussion

In this study, we examined the role of CaMKII in Ca^{2+} handling alterations of cardiomyocytes from MetS animals under the β-adrenergic response. Our results support the notion that CaMKII is autonomously activated in MetS hearts and is the underlying mechanism of the abnormal diastolic Ca^{2+} leak in the form of spontaneous Ca^{2+} waves observed in cardiomyocytes under resting conditions. Our results also demonstrate that β-adrenergic signaling pathway exacerbates the abnormal SR Ca^{2+} leak in MetS cardiomyocytes.

Our experimental MetS model was developed in rats by sucrose administration (30% in drinking water) for 16 weeks, which differs from our previous study in a MetS model at late stages [18]. In contrast with other sucrose-fed animal models [26,35], our rats displayed increased body weight, which was associated with significant abdominal fat accumulation (Table 1). The latter is a key component of our MetS model, particularly considering that obesity is a central factor of MetS pathophysiology in humans and crucial in predisposing to the development of CVD [36]. Similar to sucrose-fed rats [26], the MetS rats also developed dyslipidemia (Table 1), a metabolic condition independently related to stroke and/or myocardial infarction in MetS patients [37].

Clinical studies have also reported that MetS patients have a well-established hyper-adrenergic state that could account for CVD morbidity and mortality [7,38]. Previous reports in HTG and MetS rats reported arrhythmic events and impaired cardiac sinus rhythm recovery after *in vivo* or *ex-vivo* ischemia-reperfusion procedures [26–28]. Accordingly, MetS rats were more prompted to develop ventricular fibrillation after the administration of an arrhythmogenic cocktail (Supp. Fig 1) It is well documented that abnormal activation of CaMKII signaling pathways triggers cardiac arrhythmogenic activity in several congenital and acquired cardiac pathologies [14,39–41], and that this condition could be exacerbated

under β-adrenergic stress. Indeed, resting MetS cardiomyocytes exhibited abnormal diastolic Ca^{2+} leak mainly in the form of Ca^{2+} waves (Figure 1). Interestingly, ISO effect on Ca^{2+} spark frequency was evident in both experimental groups. It is important to note that Ca^{2+} waves contribute to diastolic Ca^{2+} leak (Figure 1D); further, Ca^{2+} waves contribute more significantly to inward NCX current, thereby promoting arrhythmogenic activity [9]. Compelling evidence shows an association between Ca^{2+} wave formation and SR Ca^{2+} content threshold, which can be shifted toward spontaneous Ca^{2+} release due to changes in RyR2 properties [42] or increased SR Ca^{2+} content [43]. However, our data do not support the latter, because SR Ca^{2+} content, measured by the delta of the amplitude of the caffeine-evoked Ca^{2+} transients, remained unmodified in MetS cardiomyocytes even in the presence of ISO (Figure 1E), as it has been demonstrated in other CVD models [22]. Ca^{2+} spark frequency and morphometric properties are determined by SR Ca^{2+} load, cytoplasmic $[Ca^{2+}]_i$, factors that control the opening and closure of the RyR2 channel; for instance, single current amplitude, RyR Ca^{2+} sensitivity, regulatory proteins, posttranslational modifications, and point mutations, among others [22,44–47]. Also, cytosolic and intra SR Ca^{2+} diffusion and clearance mechanisms are participating [44,47]. In normal cardiomyocytes and under very controlled conditions, β-adrenergic stimulus increases the potential for the RyRs to release a given amount of Ca^{2+} abruptly, as Ca^{2+} sparks [45], augmenting their frequency as it was observed in CTL+ISO and MetS+ISO cells. ISO did not modify Ca^{2+} spark amplitude in both experimental groups (Table 2), as previously reported in cardiomyocytes with similar SR Ca^{2+} load [44]. Other Ca^{2+} spark properties such as FWHM and FDHM that were expected to increase with ISO [45] in our conditions were reduced (FDHM in CTL+ISO cells) or remain similar (FWHM in both CTL+ISO and MetS+ISO cells) respect to control cells (Table 2). A possible explanation for our results in MetS cells, is that the augmented Ca^{2+} wave-mediated Ca^{2+} leak is preventing a modification in other Ca^{2+} spark characteristics.

Alterations in the properties of RyR2 are also known to trigger the occurrence of Ca^{2+} waves. Among the several post-translational modifications that the RyR2 undergoes, its phosphorylation via PKA and CaMKII is the primary mechanism for regulating its Ca^{2+} sensitivity and in situ activity. Thus, changes in RyR2 phosphorylation have been frequently associated with the occurrence of cardiac arrhythmic events [29,48]. In this regard, a study using a dog model of high-fat-induced MetS demonstrated a decrease in cardiac RyR2 activity and significantly increased phosphorylation levels at S2808 [49]. In contrast, a study with a murine MetS model (sucrose-fed) by Okatan et al., reported an increase in S2808-RyR2 phosphorylation associated with disturbances in cardiomyocyte Ca^{2+} handling, where RyR2 was more “leaky” during diastole. Further, the authors found that SERCA pump activity was depressed via a mechanism involving SERCA oxidation [35,50]. Despite these discrepancies, RyR2 phosphorylation clearly plays a crucial role in the cardiac MetS outcome. In our hands, we found only differences in S2808-RyR2 phosphorylation in the CTL condition after ISO treatment (Figure 2D), which agrees well with the considerable levels of S2808-RyR2 phosphorylation we observed under basal conditions [31,48].

In contrast, we found significant phosphorylation of the S2814-RyR2 site in MetS hearts under basal conditions (Figure 2E); this likely accounted for the increase in diastolic Ca^{2+} leak in MetS cardiomyocytes. Our results agree with previous reports associating this

specific post-translational modification with RyR2- mediated Ca^{2+} release [12,51]. Likely, in a fructose-fed rat model, S2814-RyR2 basal phosphorylation levels were increased with a clear association with abnormal diastolic Ca^{2+} leak [15]; however, no evidence of ISO effects on S2814-RyR2 phosphorylation in this metabolic model was provided. Interestingly, Bers et al., [48,52] found that ISO treatment only increased S2814-RyR phosphorylation in rat cardiomyocytes after electrical stimulation, which could help to explain why β-adrenergic stimuli did not further increase S2814-RyR2 phosphorylation levels in either MetS or CTL hearts (Figure 2E).

Some studies using various prediabetic and diabetic models reported loss of SERCA pump function [18,35,53]. In contrast, SERCA pump activity was reportedly upregulated in a fructose-induced MetS model at early stages, which was interpreted as an initial compensatory mechanism in the heart [54]. Considering that we found abnormal diastolic Ca^{2+} leak without alterations of SR Ca^{2+} content in our experimental MetS model, we hypothesized that the SERCA pump activity would be upregulated. Indeed, our data showed that SERCA pump activity was increased in MetS hearts (Figure 3A and 3B). Intriguingly, the SERCA activity of MetS hearts was quite similar to the SERCA ATPase activity determined in ISO-stimulated hearts (in both CTL and MetS conditions), though PLN phosphorylation levels were alike (Figure 4). However, it has been previously demonstrated that either PKA- or ISO-induced stimulation of SERCA ATPase activity is clearly more effective at low free Ca^{2+} concentrations (~ 0.7 μM) that at optimal free Ca^{2+} (≥ 10 μM) in cardiac SR vesicles [55,56]. Because in the present work, the experimental protocol to measure the SERCA ATPase activity was optimized to obtain the maximal hydrolytic activity (no substrate restriction, ~10 μM free Ca^{2+} concentration; and in the presence of a Ca^{2+} ionophore to dissipate the calcium gradient), we assume that any increase in PLN phosphorylation will rise SERCA ATPase activity to the maximum level, thus no gradual changes in ATPase activity would be observed. In the future, a better approach to determine the fine regulation of PLN phosphorylation on SERCA pump hydrolytic activity could be accomplished by reducing the free Ca^{2+} concentration to suboptimal levels (≤ 1 μM) in the ATPase assay.

As mentioned previously, CaMKII has several Ca^{2+} handling targets, among them PLN, which constitutes an important regulator of the SERCA pump and therefore a key component of cardiomyocyte relaxation mechanisms. Importantly, we found that PLN-Thr17 phosphorylation was augmented in MetS (Figure 4C). This finding agrees with similar results obtained in fructose-fed rats [15]; and is in disagreement with a report in sucrose-fed MetS model, where PLN phosphorylation status did not explain SERCA pump dysfunction [35].

Given that both S2814-RyR2 and T17-PLN are sites exclusively phosphorylated by CaMKII [13], the finding of higher levels of phosphorylation of these sites clearly indicates that CaMKII plays a key role in the abnormal diastolic Ca^{2+} leak and arrhythmogenic activity in MetS. We validated the contribution of CaMKII by evaluating its auto-phosphorylation state (Figure 5C). Therefore, MetS upregulates this post-translational modification, which results in the long-term potentiation of CaMKII activity—no other stimuli are required. Our results are in line with those reporting increased CaMKII auto-phosphorylation levels after a high-

carbohydrate diet [15,57]. Is important to note that autonomous activation of CaMKII by T287 auto-phosphorylation is a mechanism promoted by the frequency of the Ca^{2+} release events that prevails until the dephosphorylation of the site by PP1 or PP2a phosphatases [13]. Hence, Western blot results showed that only in the MetS condition this autonomous activation mechanism is prevalent, however this does not mean that CaMKII is not activated in other conditions.

Importantly, inhibition with the peptide AIP served as further evidence of CaMKII participation in the increased Ca^{2+} leak (Figure 6) induced by S2814 RyR phosphorylation (Supplementary Figure 5) in the MetS condition. Despite the fact that the inhibition of abnormal diastolic Ca^{2+} leak in AIP-treated MetS cardiomyocytes was not associated with disturbances in SR-Ca^{2+} load or diastolic (F_0) fluorescence (Figure 6), further investigation will be required to determine in-depth whether AIP treatment alters diastolic [Ca^{2+}].We are aware that this MetS model entails a variety of pathophysiological implications that must be approached in the future. For instance, it is well known that oxidative stress is a consequence of obesity and dyslipidemia that is associated with the cardiometabolic complications of these conditions [58]. Given that obesity and dyslipidemia are main components of our MetS model, it would be interesting to evaluate the oxidative status in the MetS cardiomyocytes, particularly of those Ca^{2+} handling related proteins susceptible to oxidative post-translational modifications (Ox-PTMs) such as the RyR and CaMKII. Oxidative stress can exacerbate SR-Ca^{2+} leak directly by enhancing RyR activity and indirectly by contributing to CaMKII autonomous activation mechanism [40,59]. Thus, it would be interesting to unveil the association of obesity-induced oxidative stress in the intracellular Ca^{2+} disturbances observed in our MetS model. However, as far as we know, T287-CaMKII autophosphorylation is primarily driven by high Ca^{2} dynamics, ruling out the participation of ROS in the autonomous activation of CaMKII in our experimental MetS model. This statement is supported by experiments in a sucrose-fed model where oxidized levels of CaMKII were not changed despite the increased ROS production [57].

Lately, abnormal CaMKII activation has been associated with diabetic cardiomyopathy and late-stage metabolic syndrome [14,18,60]. In this matter, it is worthy to mention a previous report from our group in a late-stage MetS model (30% sucrose in drinking water for 24 weeks); in which an impairment in RyR and SERCA pump activation due to decreased S2814-RyR and T17-PLN phosphorylation, respectively, was observed, in a similar way as the results in AIP-treated MetS cells, indicating a down-regulation in CaMKII activation[18]. Taken together, these results suggest a pivotal role of CaMKII in the progression of prediabetic cardiomyopathy. At early stages of MetS, when heart energy demand is still not compromised, CaMKII is upregulated; while at late stages of MetS, with marked diminution of ATP, phosphocreatine content; and creatine kinase activity [61], CaMKII is downregulated [18].

5. Conclusion

Our results support the notion that CaMKII autonomous activation in MetS hearts significantly contributes to exacerbating diastolic Ca^{2+} leak (mainly in the form of Ca^{2+} waves) after β-adrenergic stimulation. Main findings of this work are: 1) abnormal Ca^{2+}

wave-driven diastolic Ca^{2+} leak in MetS cardiomyocytes is exacerbated after β-adrenergic stimulation; 2) RyR2 and PLN phosphorylation at CaMKII target sites underlie augmented diastolic Ca^{2+} leak in MetS cardiomyocytes; 3) auto-phosphorylation of T287-CaMKII accounts for CaMKII autonomous activation in MetS hearts; 4) conversely, pharmacological AIP-induced CaMKII inhibition reduces diastolic Ca^{2+} leak in myocytes from MetS hearts. Finally, exacerbated CaMKII activation in the heart could account for detrimental β-adrenergic responses at early stages of MetS.

Supplementary Material

Refer to Web version on PubMed Central for supplementary material.

Acknowledgments

We deeply thank Dr. Agustín Guerrero-Hernández (Department of Biochemistry, Cinvestav-IPN, México) for providing us with the facilities to perform the determination of basal $[Ca^{2+}]_i$ in Fura 2-loaded cardiomyocytes. We are very grateful to Dr. Jean Pierre Benitah (UMR-1180 LabEx LERMIT Inserm, France) for his invaluable recommendations to our work. We thank Dr. E. Michelle Frank (The Well-Tempered Word LLC) for critical reading of the manuscript. We also wish to acknowledge the technical assistance of Juan Carlos García Torres for the care and handling of rats.

Funding

This work was partially supported by Fundación Miguel Alemán A.C., and Fondo SEP-Cinvestav approved project #601410 FIDSC 2018/2 to R, A; by a PRODEP-SEP grant to the Academic Group CINVESTAV-CA-10, ID 28915/2018 and by NIH grants R01-HL055438 and R01-HL134344 to V, HH. R, A was a COMEXUS-Fulbright Fellow to perform a research stay at Héctor H. Valdivia laboratory (Center for Arrhythmia Research, University of Michigan Ann Arbor, MI, USA); R-G, T and L-G, H were CONACYT Ph.D. fellows.

Abbreviations

AIP	Autocamptide-2-related inhibitory peptide
CaMKII	Ca^{2+}/calmodulin-dependent protein kinase II
CICR	Calcium-induced calcium release
CTL	Control
CVD	Cardiovascular disease
EADs	Early after depolarizations
ECC	Excitation-contraction coupling
GAPDH	Glyceraldehyde-3-phosphate dehydrogenase
HDL	High-density lipoprotein
ISO	Isoproterenol
LV	Left ventricle
MetS	Metabolic Syndrome
NCX	Na^+/Ca^{2+} exchanger

PKA	Protein Kinase A
PLN	Phospholamban
RyR	Ryanodine receptor
SERCA	Sarco/Endoplasmic reticulum Ca^{2+} ATPase
SR	Sarcoplasmic reticulum

References

[1]. Alberti KGMM, Eckel RH, Grundy SM, Zimmet PZ, Cleeman JI, Donato KA, Fruchart JC, James WPT, Loria CM, Smith SC, Harmonizing the metabolic syndrome: A joint interim statement of the international diabetes federation task force on epidemiology and prevention; National heart, lung, and blood institute; American heart association; World heart federation; International, Circulation. 120 (2009) 1640–1645. [PubMed: 19805654]

[2]. Arellano-Campos O, V Gómez-Velasco D, Bello-Chavolla OY, Cruz-Bautista I, Melgarejo-Hernandez MA, Muñoz-Hernandez L, Guillén LE, Garduño-Garcia J, Alvirde U, Ono-Yoshikawa Y, Choza-Romero R, Sauque-Reyna L, Garay-Sevilla ME, Malacara-Hernandez J, Tusie-Luna MT, Gutierrez-Robledo LM, Gómez-Pérez FJ, Rojas R, Aguilar-Salinas CA, Development and validation of a predictive model for incident type 2 diabetes in middle-aged Mexican adults: the metabolic syndrome cohort, BMC Endocr. Disord 19 (2019) 41. [PubMed: 31030672]

[3]. Tune JD, Goodwill AG, Sassoon DJ, Mather KJ, Cardiovascular consequences of metabolic syndrome, Transl. Res 183 (2017) 57–70. [PubMed: 28130064]

[4]. Grundy SM, Brewer HB, Cleeman JI, Smith SC, Lenfant C, Definition of Metabolic Syndrome: Report of the National Heart, Lung, and Blood Institute/American Heart Association Conference on Scientific Issues Related to Definition, Circulation. 109 (2004) 433–438. [PubMed: 14744958]

[5]. Alberti KGMM, Zimmet P, Shaw J, The metabolic syndrome - A new worldwide definition, Lancet. 366 (2005) 1059–1062. [PubMed: 16182882]

[6]. Cabré JJ, Martín F, Costa B, Pīol JL, Llor JL, Ortega Y, Basora J, Baldrich M, Solà R, Daniel J, Hernández JM, Saumell J, Bladé J, Sagarra R, Basora T, Montãés D, Frigola JL, Donado-Mazarrón A, García-Vidal MT, Sánchez-Oro I, De Magrîà JM, Urbaneja A, Barrio F, Vizcaíno J, Sabaté JM, Pascual I, Revuelta V, Metabolic syndrome as a cardiovascular disease risk factor: Patients evaluated in primary care, BMC Public Health. 8 (2008) 1–12. [PubMed: 18173844]

[7]. Dincer UD, Cardiac ryanodine receptor in metabolic syndrome: is JTV519 (K201) future therapy?, Diabetes. Metab. Syndr. Obes 5 (2012) 89–99. [PubMed: 22563249]

[8]. Pereira L, Ruiz-Hurtado G, Rueda A, Mercadier J-J, Benitah J-P, Gómez AM, Calcium signaling in diabetic cardiomyocytes., Cell Calcium. 56 (2014) 372–80. [PubMed: 25205537]

[9]. Bers DM, Cardiac sarcoplasmic reticulum calcium leak: basis and roles in cardiac dysfunction., Annu. Rev. Physiol 76 (2014) 107–27. [PubMed: 24245942]

[10]. Eisner D, Calcium in the heart: From physiology to disease, Exp. Physiol 99 (2014) 1273–1282. [PubMed: 25128325]

[11]. Kumari N, Gaur H, Bhargava A, Cardiac voltage gated calcium channels and their regulation by β-adrenergic signaling, Life Sci. 194 (2018) 139–149. [PubMed: 29288765]

[12]. Grimm M, Ling H, Willeford A, Pereira L, Gray CBB, Erickson JR, Sarma S, Respress JL, Wehrens XHT, Bers DM, Brown JH, CaMKIIδ mediates β-adrenergic effects on RyR2 phosphorylation and SR Ca2+ leak and the pathophysiological response to chronic β-adrenergic stimulation, J. Mol. Cell. Cardiol 85 (2015) 282–291. [PubMed: 26080362]

[13]. Erickson JR, Mechanisms of CaMKII Activation in the Heart, Front. Pharmacol 5 (2014) 59. [PubMed: 24765077]

[14]. Erickson JR, Pereira L, Wang L, Han G, Ferguson A, Dao K, Copeland RJ, Despa F, Hart GW, Ripplinger CM, Bers DM, Diabetic hyperglycaemia activates CaMKII and arrhythmias by O-linked glycosylation, Nature. 502 (2013) 372–376. [PubMed: 24077098]

[15]. Sommese L, Valverde CA, Blanco P, Castro MC, Rueda OV, Kaetzel M, Dedman J, Anderson ME, Mattiazzi A, Palomeque J, Ryanodine receptor phosphorylation by CaMKII promotes spontaneous Ca2+ release events in a rodent model of early stage diabetes: The arrhythmogenic substrate, Int. J. Cardiol 202 (2016) 394–406. [PubMed: 26432489]

[16]. Federico M, Portiansky EL, Sommese L, Alvarado FJ, Blanco PG, Zanuzzi CN, Dedman J, Kaetzel M, Wehrens XHT, Mattiazzi A, Palomeque J, Calcium-calmodulin-dependent protein kinase mediates the intracellular signalling pathways of cardiac apoptosis in mice with impaired glucose tolerance, J. Physiol 595 (2017) 4089–4108. [PubMed: 28105734]

[17]. De Koninck P, Schulman H, Meyer T, Stryer L, Berridge MJ, Clapham DE, Berridge MJ, Malinow R, Schulman H, Tsien RW, Silva AJ, Stevens CF, Tonegawa S, Wang Y, Deisseroth K, Bito H, Schulman H, Tsien RW, Lisman JE, Soderling TR, Braun AP, Schulman H, Hanson PI, Schulman H, Meyer T, Hanson PI, Stryer L, Schulman H, Hanson PI, Meyer T, Stryer L, Schulman H, Michelson S, Schulman H, Dosemeci A, Albers RW, Mayer P, Mohlig M, Schatz H, Pfeiffer A, Hanson PI, Kapiloff MS, Lou LL, Rosenfeld MG, Schulman H, Brocke L, Srinivasan M, Schulman H, Mukherji S, Soderling TR, Baitinger C, Alderton J, Poenie M, Schulman H, Steinhardt RA, Klee CB, Luby-Phelps K, Hori M, Phelps JM, Won D, MacNicol M, Jefferson AB, Schulman H, Fukunaga K, Stoppini L, Miyamoto E, Muller D, Barria A, Muller D, Derkach V, Griffith LC, Soderling TR, Molloy SS, Kennedy MB, Ocorr KA, Schulman H, Miller SG, Kennedy MB, Huerta PT, Lisman JE, Frey U, Morris RGM, Hanson PI, Schulman H, Kanaseki T, Ikeuchi Y, Sugiura H, Yamauchi T, Sensitivity of CaM kinase II to the frequency of Ca2+ oscillations., Science. 279 (1998) 227–30. [PubMed: 9422695]

[18]. Fernández-Miranda G, Romero-Garcia T, Barrera-Lechuga TP, Mercado-Morales M, Rueda A, Impaired Activity of Ryanodine Receptors Contributes to Calcium Mishandling in Cardiomyocytes of Metabolic Syndrome Rats, Front. Physiol 10 (2019) 520. [PubMed: 31114513]

[19]. de Alba-Aguayo DR, Pavón N, Mercado-Morales M, Miranda-Saturnino M, López-Casamichana M, Guerrero-Hernández A, Rueda A, Increased calcium leak associated with reduced calsequestrin expression in hyperthyroid cardiomyocytes, Cell Calcium. 62 (2017) 29–40. [PubMed: 28169003]

[20]. Biesmans L, Macquaide N, Heinzel FR, Bito V, Smith GL, Karin R, Sipido KR, Subcellular heterogeneity of ryanodine receptor properties in ventricular myocytes with low T-tubule density., PLoS One. 6 (2011) e25100. [PubMed: 22022376]

[21]. Grynkiewicz G, Poenie M, Tsien RY, A new generation of Ca2+ indicators with greatly improved fluorescence properties., J. Biol. Chem 260 (1985) 3440–50. [PubMed: 3838314]

[22]. Fernández-Velasco M, Rueda A, Rizzi N, Benitah J-P, Colombi B, Napolitano C, Priori SG, Richard S, Gómez AM, Increased Ca2+ sensitivity of the ryanodine receptor mutant RyR2R4496C underlies catecholaminergic polymorphic ventricular tachycardia., Circ. Res 104 (2009) 201–9, 12p following 209. [PubMed: 19096022]

[23]. Bartolommei G, Moncelli MR, Tadini-buoninsegni F, A Method to Measure Hydrolytic Activity of Adenosinetriphosphatases (ATPases), PLoS One. 8 (2013) e58615. [PubMed: 23472215]

[24]. Salazar MR, Carbajal HA, Espeche WG, Aizpurúa M, Leiva Sisnieguez CE, Leiva Sisnieguez BC, March CE, Stavile RN, Balbín E, Reaven GM, Use of the plasma triglyceride/high-density lipoprotein cholesterol ratio to identify cardiovascular disease in hypertensive subjects, J. Am. Soc. Hypertens 8 (2014) 724–731. [PubMed: 25418494]

[25]. Landstrom AP, Dobrev D, Wehrens XHT, Calcium Signaling and Cardiac Arrhythmias., Circ. Res 120 (2017) 1969–1993. [PubMed: 28596175]

[26]. Cárdenas G, Carlos Torres J, Zamora J, Pérez I, Baños G, Isolated heart function after ischemia and reperfusion in sucrose-fed rats: influence of gender and treatment., Clin. Exp. Hypertens 28 (2006) 85–107. [PubMed: 16546836]

[27]. Carvajal K, El Hafidi M, Baños G, Myocardial damage due to ischemia and reperfusion in hypertriglyceridemic and hypertensive rats: participation of free radicals and calcium overload., J. Hypertens 17 (1999) 1607–16. [PubMed: 10608475]

[28]. Fernández-Sada E, Torres-Quintanilla A, Silva-Platas C, García N, Willis BC, Rodríguez-Rodríguez C, De la Peña E, Bernal-Ramírez J, Treviño-Saldaña N, Oropeza-Almazán Y, Castillo EC, Elizondo-Montemayor L, Carvajal K, García-Rivas G, Proinflammatory Cytokines Are Soluble Mediators Linked with Ventricular Arrhythmias and Contractile Dysfunction in a Rat Model of Metabolic Syndrome, Oxid. Med. Cell. Longev 2017 (2017) 1–12.

[29]. Camors E, Valdivia HH, CaMKII regulation of cardiac ryanodine receptors and inositol triphosphate receptors., Front. Pharmacol 5 (2014) 101. [PubMed: 24847270]

[30]. Li J, Imtiaz MS, Beard NA, Dulhunty AF, Thorne R, vanHelden DF, Laver DR, ß-Adrenergic Stimulation Increases RyR2 Activity via Intracellular Ca2+ and Mg2+ Regulation, PLoS One. 8 (2013).

[31]. Rodriguez P, Bhogal MS, Colyer J, Stoichiometric Phosphorylation of Cardiac Ryanodine Receptor on Serine 2809 by Calmodulin-dependent Kinase II and Protein Kinase A, J. Biol. Chem 278 (2003) 38593–38600. [PubMed: 14514795]

[32]. Kranias EG, Hajjar RJ, Modulation of cardiac contractility by the phopholamban/SERCA2a regulatome, Circ. Res 110 (2012) 1646–1660. [PubMed: 22679139]

[33]. Mattiazzi A, Kranias EG, The role of CaMKII regulation of phospholamban activity in heart disease, Front. Pharmacol 5 (2014) 1–11. [PubMed: 24478702]

[34]. Vest RS, Davies KD, O'Leary H, Port JD, Bayer KU, Dual Mechanism of a Natural CaMKII Inhibitor, Mol. Biol. Cell 18 (2007) 5024–5033. [PubMed: 17942605]

[35]. Balderas-Villalobos J, Molina-Muñoz T, Mailloux-Salinas P, Bravo G, Carvajal K, Gómez-Viquez NL, Oxidative stress in cardiomyocytes contributes to decreased SERCA2a activity in rats with metabolic syndrome., Am. J. Physiol. Heart Circ. Physiol 305 (2013) H1344–53. [PubMed: 23997093]

[36]. Han TS, Lean ME, A clinical perspective of obesity, metabolic syndrome and cardiovascular disease, JRSM Cardiovasc. Dis 5 (2016) 1–13.

[37]. Ninomiya JK, L'Italien G, Criqui MH, Whyte JL, Gamst A, Chen RS, Association of the Metabolic Syndrome with History of Myocardial Infarction and Stroke in the Third National Health and Nutrition Examination Survey, Circulation. 109 (2004) 42–46. [PubMed: 14676144]

[38]. De Pergola G, Giorgino F, Benigno R, Guida P, Giorgino R, Independent Influence of Insulin, Catecholamines, and Thyroid Hormones on Metabolic Syndrome, Obesity. 16 (2008) 2405–2411. [PubMed: 18719673]

[39]. Koval OM, Snyder JS, Wolf RM, Pavlovicz RE, Glynn P, Curran J, Leymaster ND, Dun W, Wright PJ, Cardona N, Qian L, Mitchell CC, Boyden PA, Binkley PF, Li C, Anderson ME, Mohler PJ, Hund TJ, Ca2+/calmodulin-dependent protein kinase ii-based regulation of voltage-gated na+ channel in cardiac disease, Circulation. 126 (2012) 2084–2094. [PubMed: 23008441]

[40]. Swaminathan PD, Purohit A, Soni S, Voigt N, Singh MV, Glukhov AV, Gao Z, He BJ, Luczak ED, Joiner MLA, Kutschke W, Yang J, Donahue JK, Weiss RM, Grumbach IM, Ogawa M, Chen PS, Efimov I, Dobrev D, Mohler PJ, Hund TJ, Anderson ME, Oxidized CaMKII causes cardiac sinus node dysfunction in mice, J. Clin. Invest 121 (2011) 3277–3288. [PubMed: 21785215]

[41]. Liu N, Ruan Y, Denegri M, Bachetti T, Li Y, Colombi B, Napolitano C, Coetzee WA, Priori SG, Calmodulin kinase II inhibition prevents arrhythmias in RyR2R4496C+/− mice with catecholaminergic polymorphic ventricular tachycardia, J. Mol. Cell. Cardiol 50 (2011) 214–222. [PubMed: 20937285]

[42]. Venetucci LA, Trafford AW, Eisner DA, Increasing ryanodine receptor open probability alone does not produce arrhythmogenic calcium waves: Threshold sarcoplasmic reticulum calcium content is required, Circ. Res 100 (2007) 105–111. [PubMed: 17110597]

[43]. Jiang D, Xiao B, Yang D, Wang R, Choi P, Zhang L, Cheng H, Chen SRW, RyR2 mutations linked to ventricular tachycardia and sudden death reduce the threshold for store-overload-induced Ca2+ release (SOICR)., Proc. Natl. Acad. Sci. U. S. A 101 (2004) 13062–7. [PubMed: 15322274]

[44]. Gómez AM, Cheng H, Lederer WJ, Bers DM, Ca2+ diffusion and sarcoplasmic reticulum transport both contribute to [Ca2+](i) decline during Ca2+ sparks in rat ventricular myocytes, J. Physiol 496 (1996) 575–581. [PubMed: 8910239]

[45]. Santiago DJ, Ríos E, Shannon TR, Isoproterenol increases the fraction of spark-dependent RyR-mediated leak in ventricular myocytes, Biophys. J 104 (2013) 976–985. [PubMed: 23473480]

[46]. Guo T, Gillespie D, Fill M, Ryanodine receptor current amplitude controls Ca2+ sparks in cardiac muscle., Circ. Res 111 (2012) 28–36. [PubMed: 22628577]

[47]. Bovo E, Mazurek SR, Fill M, V Zima A, Cytosolic Ca2+ buffering determines the intra-SR Ca2+ concentration at which cardiac Ca2+ sparks terminate, Cell Calcium. 58 (2015) 246–253. [PubMed: 26095947]

[48]. Huke S, Bers DM, Ryanodine receptor phosphorylation at Serine 2030, 2808 and 2814 in rat cardiomyocytes., Biochem. Biophys. Res. Commun 376 (2008) 80–5. [PubMed: 18755143]

[49]. Dincer UD, Araiza A, Knudson JD, Shao CH, Bidasee KR, Tune JD, Dysfunction of cardiac ryanodine receptors in the metabolic syndrome, J. Mol. Cell. Cardiol 41 (2006) 108–114. [PubMed: 16793060]

[50]. Okatan EN, Durak AT, Turan B, Electrophysiological basis of metabolic-syndrome-induced cardiac dysfunction, Can. J. Physiol. Pharmacol 94 (2016) 1064–1073. [PubMed: 27322594]

[51]. Respress JL, Van Oort RJ, Li N, Rolim N, Dixit SS, Dealmeida A, Voigt N, Lawrence WS, Skapura DG, Skårdal K, Wisløff U, Wieland T, Ai X, Pogwizd SM, Dobrev D, Wehrens XHT, Role of RyR2 phosphorylation at S2814 during heart failure progression, Circ. Res 110 (2012) 1474–1483. [PubMed: 22511749]

[52]. Huke S, Bers DM, Temporal dissociation of frequency-dependent acceleration of relaxation and protein phosphorylation by CaMKII., J. Mol. Cell. Cardiol 42 (2007) 590–9. [PubMed: 17239900]

[53]. Zarain-Herzberg A, García-Rivas G, Estrada-Avilés R, Regulation of SERCA pumps expression in diabetes, Cell Calcium. 56 (2014) 302–310. [PubMed: 25270119]

[54]. Miklós Z, Kemecsei P, Bíró T, Marincsák R, Tóth BI, Op den Buijs J, Benis É, Drozgyik A, Ivanics T, Early cardiac dysfunction is rescued by upregulation of SERCA2a pump activity in a rat model of metabolic syndrome., Acta Physiol. (Oxf) 205 (2012) 381–93. [PubMed: 22289164]

[55]. Kranias EG, Mandel F, Wang T, Schwartz A, Mechanism of the Stimulation of Calcium Ion Dependent Adenosine Triphosphatase of Cardiac Sarcoplasmic Reticulum by Adenosine 3', 5'-Monophosphate Dependent Protein Kinase, Biochemistry. 19 (1980) 5434–5439. [PubMed: 6255993]

[56]. Lindemann JP, Jones LR, Hathaway DR, Henry BG, Watanabe AM, β-Adrenergic stimulation of phospholamban phosphorylation and Ca 2+-ATPase activity in guinea pig ventricles, J. Biol. Chem 258 (1983) 464–471. [PubMed: 6217205]

[57]. Roe ND, He EY, Wu Z, Ren J, Folic acid reverses nitric oxide synthase uncoupling and prevents cardiac dysfunction in insulin resistance: Role of Ca2+/calmodulin-activated protein kinase II, Free Radic. Biol. Med 65 (2013) 234–243. [PubMed: 23820268]

[58]. Manna P, Jain SK, Obesity, Oxidative Stress, Adipose Tissue Dysfunction, and the Associated Health Risks: Causes and Therapeutic Strategies, Metab. Syndr. Relat. Disord 13 (2015) 423–444. [PubMed: 26569333]

[59]. Oda T, Yang Y, Uchinoumi H, Thomas DD, Chen-Izu Y, Kato T, Yamamoto T, Yano M, Cornea RL, Bers DM, Oxidation of ryanodine receptor (RyR) and calmodulin enhance Ca release and pathologically alter, RyR structure and calmodulin affinity, J. Mol. Cell. Cardiol 85 (2015) 240–248. [PubMed: 26092277]

[60]. Hegyi B, Bers DM, Bossuyt J, CaMKII signaling in heart diseases: Emerging role in diabetic cardiomyopathy, J. Mol. Cell. Cardiol 127 (2019) 246–259. [PubMed: 30633874]

[61]. Carvajal K, Baños G, Moreno-Sánchez R, Impairment of glucose metabolism and energy transfer in the rat heart., Mol. Cell. Biochem 249 (2003) 157–65. [PubMed: 12956411]

HIGHLIGHTS

- MetS cardiomyocytes show increased diastolic Ca^{2+} leak under basal conditions.
- Diastolic Ca^{2+} leak of Metabolic Syndrome (MetS) cardiomyocytes is exacerbated under β-adrenergic stimulation.
- Enhanced RyR and PLN basal phosphorylation by CaMKII underlies abnormal Ca^{2+} leak associated with MetS condition.
- Autonomous activation of CaMKII is involved in Ca^{2+} disturbances as evidenced by AIP reversion.

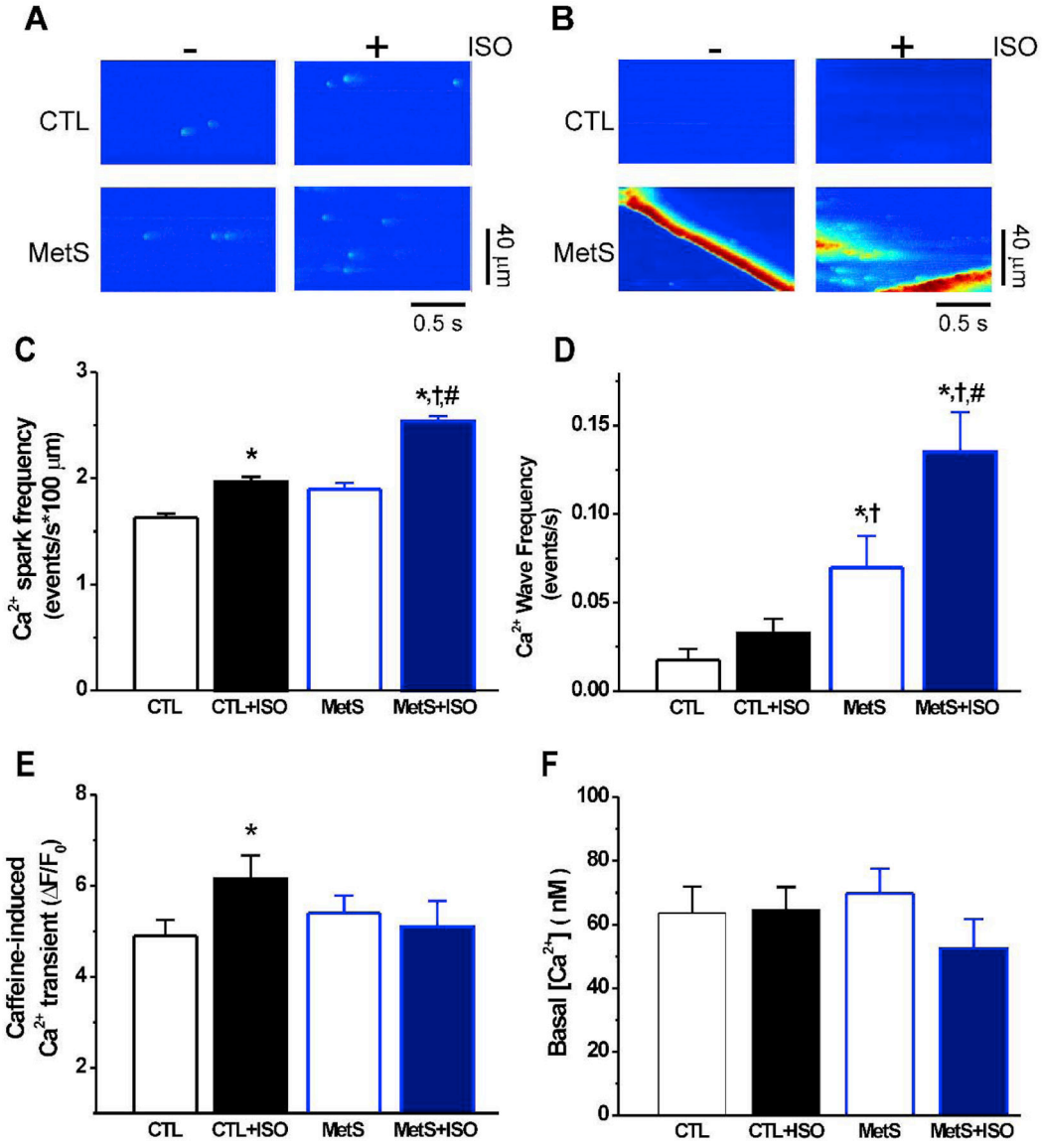

Figure 1. Exacerbated diastolic Ca^{2+} leak induced by the β-adrenergic stimulus in isolated MetS cardiomyocytes.

Representative pseudo-colored confocal images of Ca^{2+} spark (**A**) and Ca^{2+} waves (**B**) recorded in quiescent Fluo-3 loaded cardiomyocytes from CTL and MetS rats in the presence of isoproterenol (ISO, 100 nM) or in its absence. **C.** Bar graph of average Ca^{2+} spark frequency. **D.** Ca^{2+} wave frequency (events/s). **E.** Caffeine-evoked Ca^{2+} transient amplitude ($\Delta F/F_0$) of Fluo-3 loaded cardiomyocytes from CTL and MetS rats, perfused with recording solution in the presence of isoproterenol (ISO, 100 nM) or in its absence. **F.** Bar graph of diastolic $[Ca^{2+}]_i$ determined in cardiomyocytes loaded with Fura-2 of CTL and MetS rats before and after ISO administration. All values are presented as mean ± SE. Ca^{2+} sparks and Ca^{2+} waves data are obtained from n=30 cells from N= 6 rats for each experimental condition. Caffeine-evoked Ca^{2+} transient data are obtained from n_{CTL}= 16 cells, $n_{CTL+ISO}$= 11 cells, n_{MetS}= 13 cells and $n_{MetS+ISO}$= 9 cells, from N = 4 rats for each experimental condition. $[Ca^{2+}]_i$ data are obtained from n_{CTL}= 9 cells, $n_{CTL+ISO}$= 8 cells,

n_{MetS}= 10 cells and $n_{MetS+ISO}$= 8 cells, from N = 3 rats for each experimental condition. *$P \leq 0.05$ with respect to the CTL group, † $P \leq 0.05$ with respect to the CTL+ISO group and # $P \leq 0.05$ with respect to the MetS group.

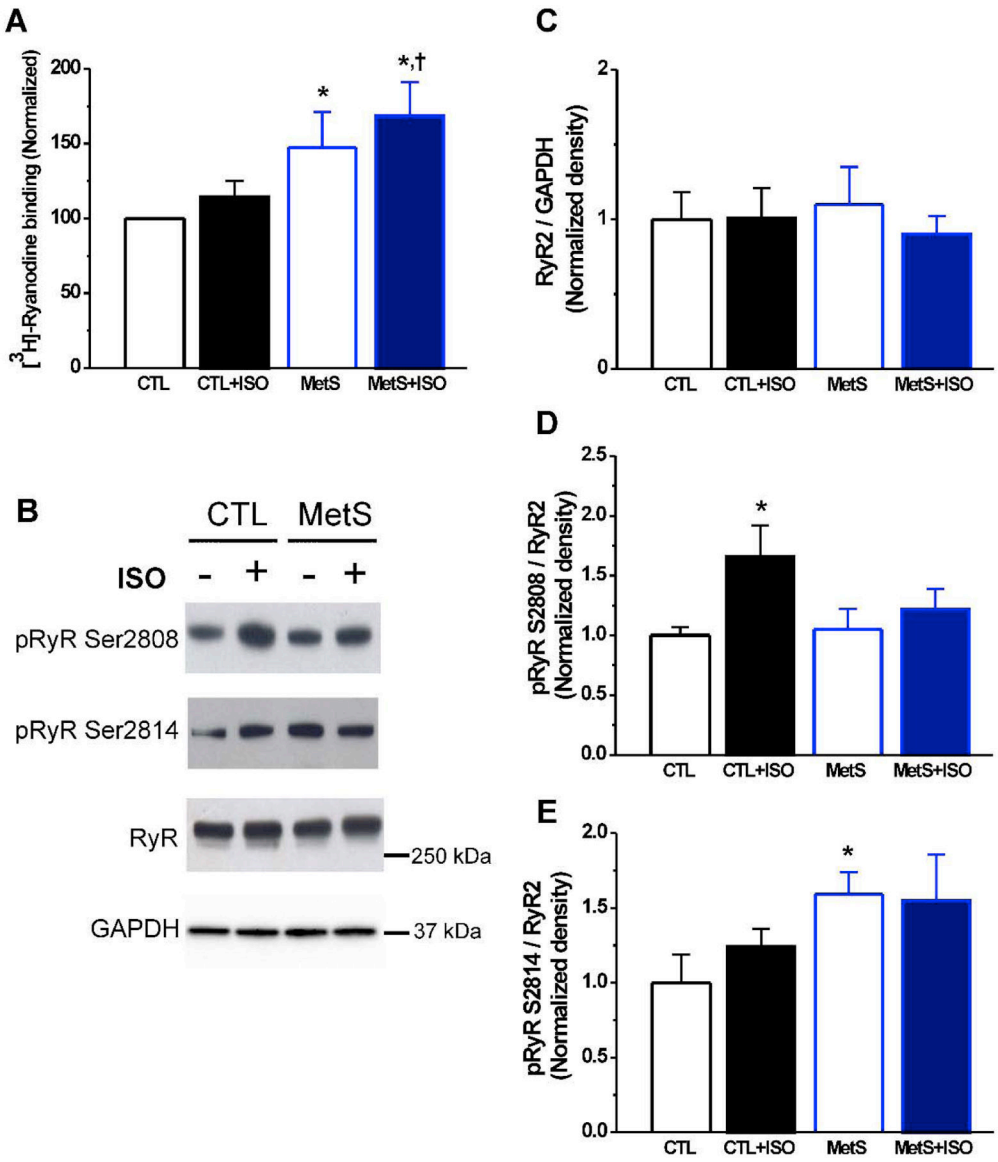

Figure 2. Increased activity of Ryanodine Receptors in MetS associated with its phosphorylation levels.

A. Normalized [^{3}H]-Ryanodine binding Bmax determined at pCa 5, pH 7.2 in CTL and MetS heart homogenates in the presence (1 μM) or absence of isoproterenol (ISO). **B.** Representative Western Blot images of total and phosphorylated RyR2 at S2808, S2814 and GAPDH, obtained from heart homogenates from CTL and MetS rats in the presence (1 μM) or absence of ISO. **C.** Total ryanodine receptor (RyR) expression normalized against corresponding GAPDH from N = 5 rats for each experimental condition. **D.** Phosphorylation levels of RyR at S2808 normalized against corresponding total RyR from N = 6 rats for each experimental condition. **E.** Phosphorylation levels of RyR at S2814 normalized against corresponding total RyR from N= 5 rats for each experimental condition. Data are expressed as mean ± SE. *$P \leq 0.05$ with respect to CTL group and † $P \leq 0.05$ with respect to the CTL + ISO group.

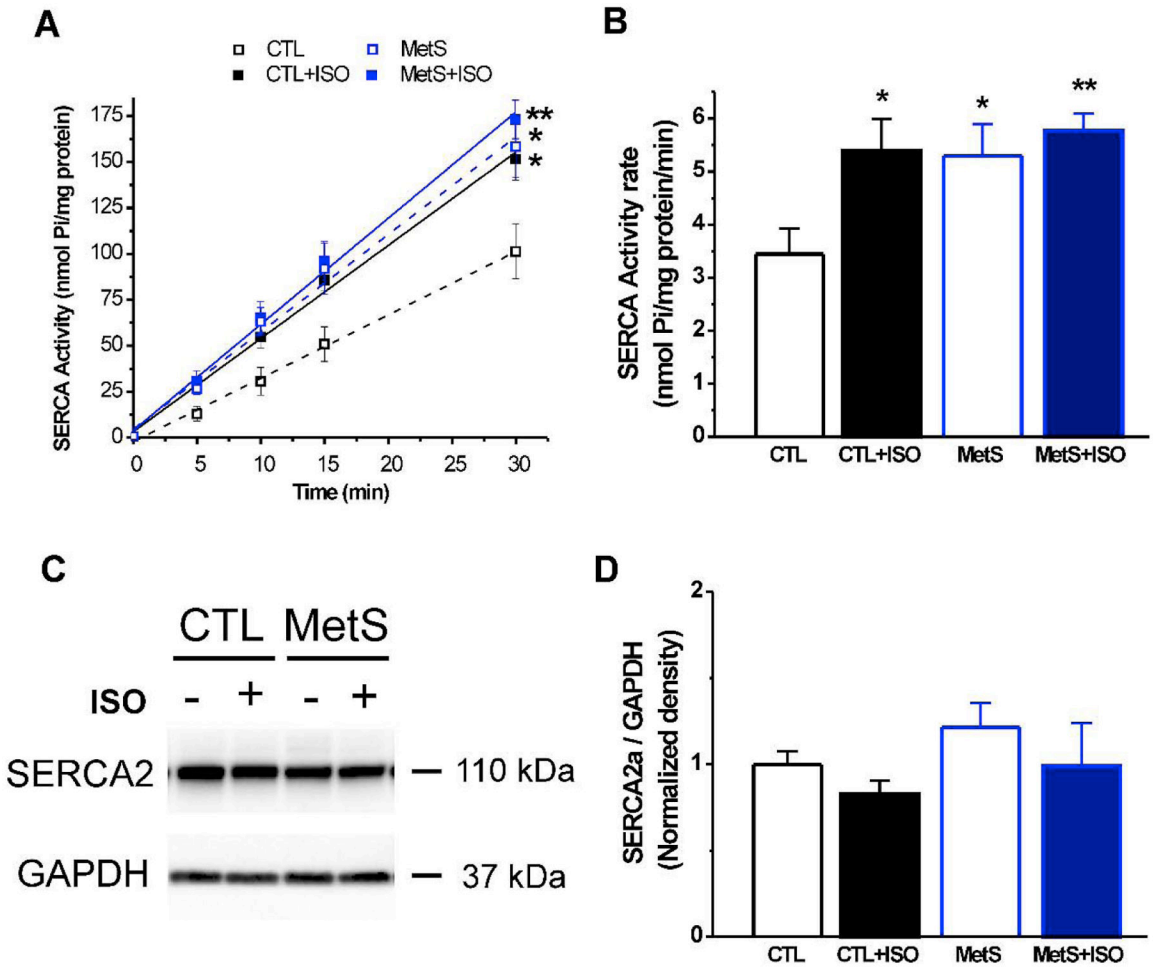

Figure 3. SERCA pump ATPase activity is increased in MetS hearts under resting conditions.

A. SERCA pump ATPase hydrolytic activity evaluated by enzymatic assay in heart homogenates of CTL and MetS rats in the presence (1 μM) or absence of isoproterenol (ISO) **B.** Bar graph of SERCA2 pump reaction rate obtained from enzymatic assay. **C.** SERCA2 protein expression normalized against corresponding GAPDH and representative Western blot. Data are expressed as mean ± SE, N= 5 rats for each experimental condition. *$P \leq 0.05$ and **$P \leq 0.001$ respect to the CTL group.

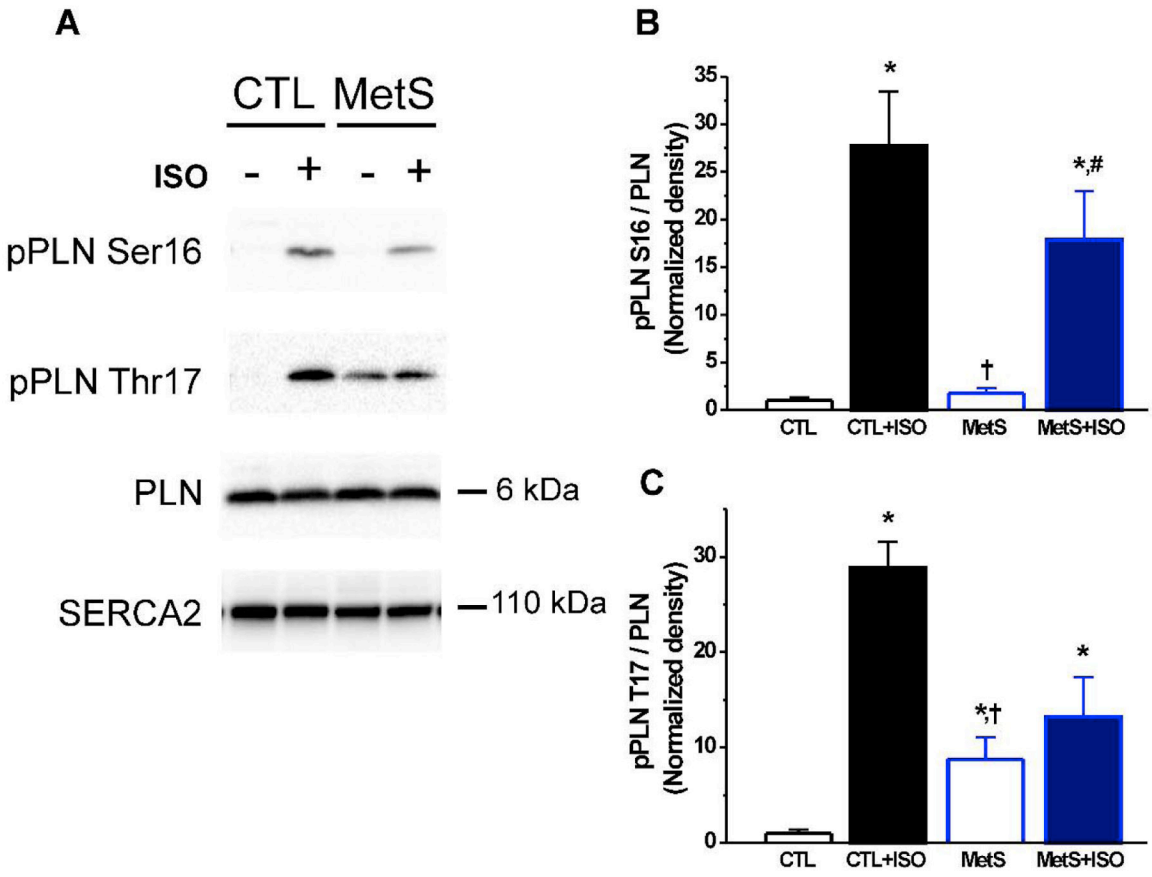

Figure 4. Augmented T17-PLN phosphorylation in MetS.

A. Representative Western Blot images of total SERCA2, PLN, and phosphorylated PLN at S16 and T17, obtained from heart homogenates from CTL and MetS rats in the presence (1 μM) or absence of isoproterenol (ISO). **B.** Phosphorylation levels of PLN at S16 normalized against corresponding total PLN. **C.** Phosphorylation levels of PLN at T17 normalized against corresponding total PLN. Data are expressed as mean ± SE, N= 5 animals for each experimental condition. * $P \leq 0.05$ with respect to the CTL group † $P \leq 0.05$ with respect to the CTL + ISO group, and # $P \leq 0.05$ with respect to the MetS group.

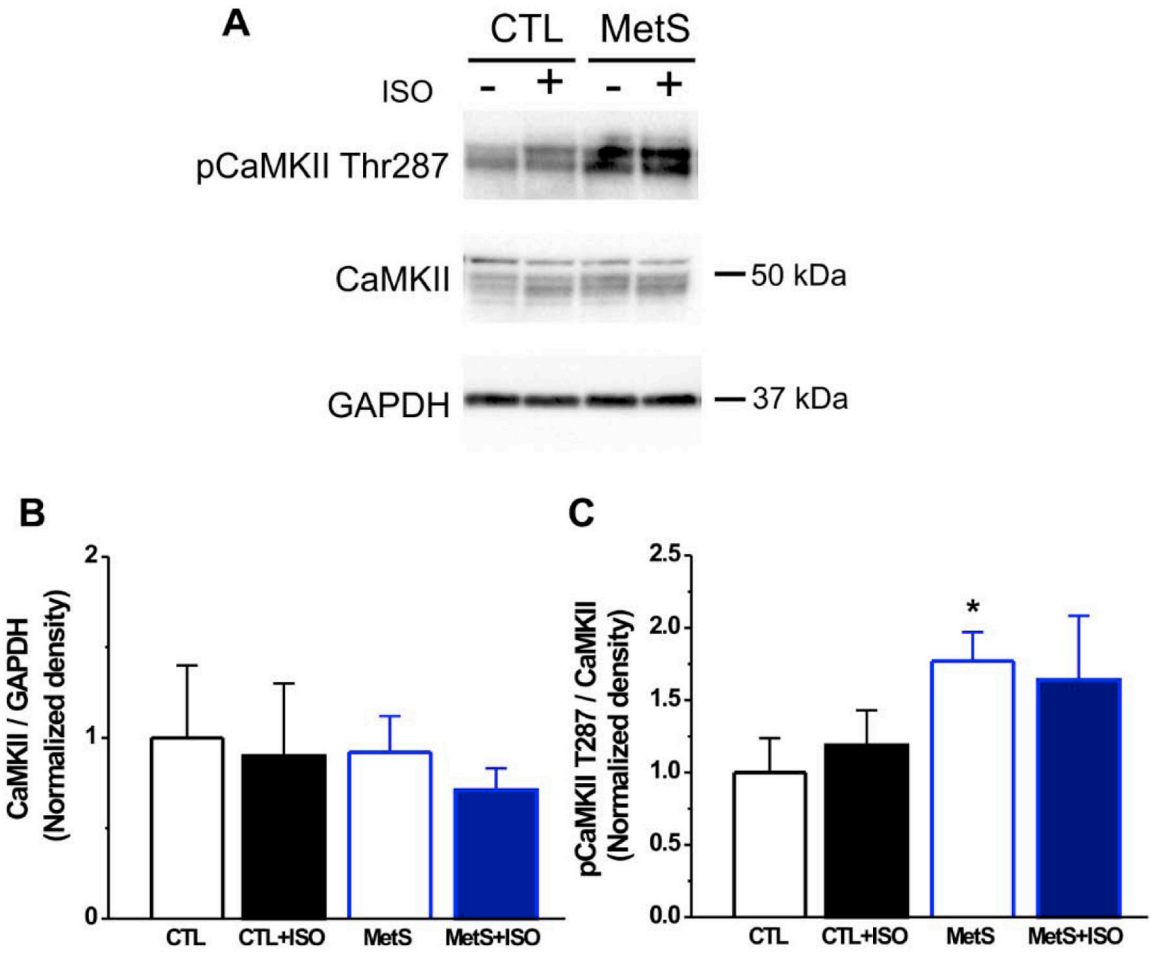

Figure 5. Autonomous activation of CaMKII is increased in MetS hearts and is unchanged by ISO.

A. Representative Western Blot images of total and phosphorylated CaMKII at T287 and GAPDH, obtained from heart homogenates from CTL and MetS rats in the presence (1 μM) or absence of isoproterenol (ISO). **B.** CaMKII protein expression normalized against corresponding GAPDH **C.** Phosphorylation levels of CaMKII at T287 normalized against corresponding total CaMKII. Data are expressed as mean ± SE, N= 5 animals for each experimental condition. *$P \leq 0.05$ with respect to the CTL group.

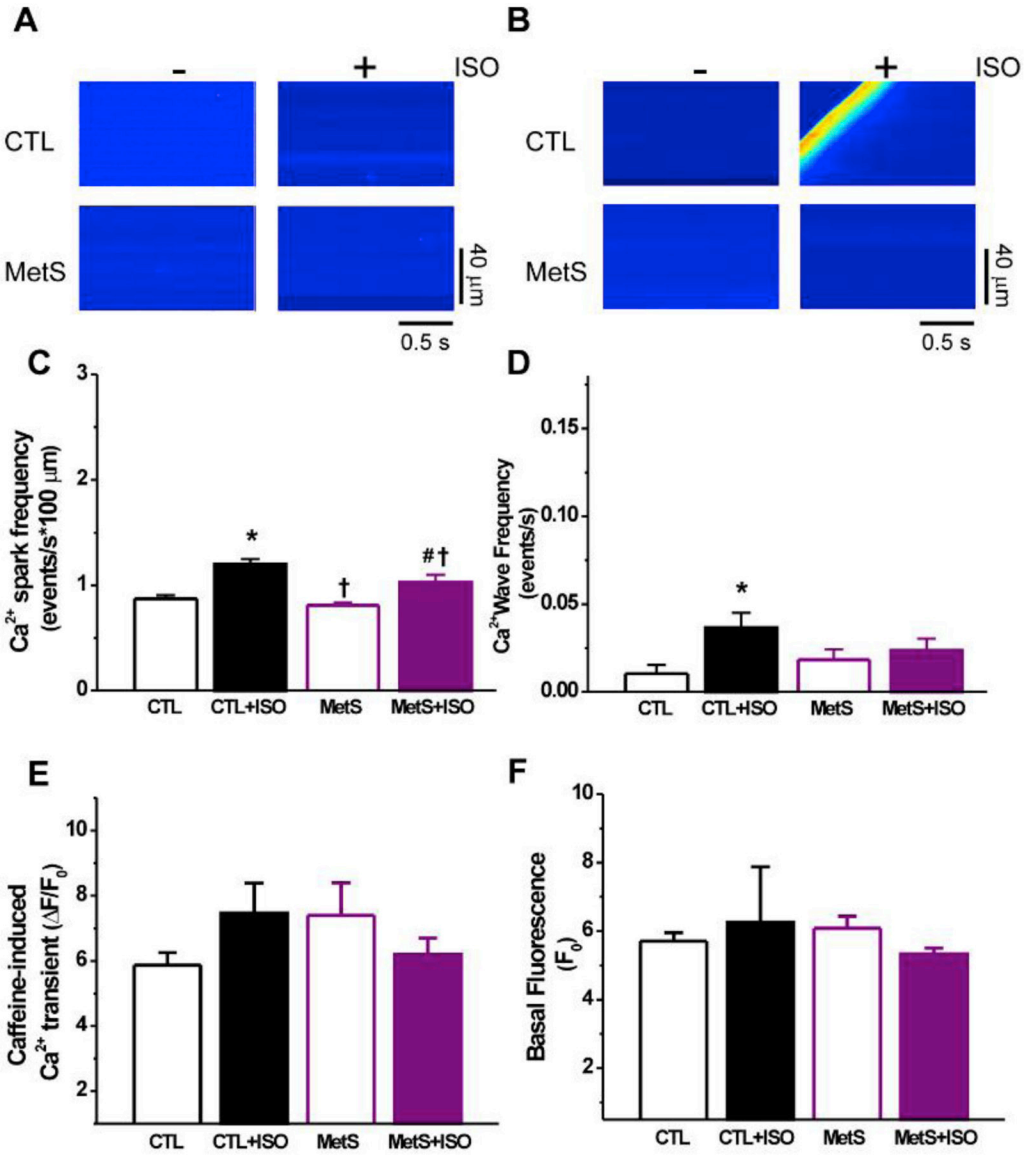

Figure 6. Incubation with AIP prevents exacerbated diastolic Ca^{2+} leak induced by the β-adrenergic stimulus in isolated MetS cardiomyocytes.

Representative pseudo-colored confocal images of Ca^{2+} sparks (**A**) and Ca^{2+} waves (**B**) recorded in quiescent Fluo-3 loaded cardiomyocytes from CTL and MetS rats pre-incubated with AIP 10 μM, in the presence or absence of isoproterenol (ISO, 100 nM). Bar graphs of Ca^{2+} spark frequencies (**C**, in events/s * 100 μm) and Ca^{2+} wave frequencies (**D**, events/s) for the different experimental conditions. **E.** Caffeine-evoked Ca^{2+} transient amplitude ($\Delta F/F_0$) of Fluo 3-loaded cardiomyocytes from CTL and MetS rats pretreated with AIP (10 μM), and perfused with recording solution in the presence of isoproterenol (ISO, 100 nM) or in its absence. **F.** Bar graph of basal fluorescence (F_0) determined in Fluo 3-loaded, AIP-treated cardiomyocytes of CTL and MetS rats before and after ISO administration. All values are presented as mean ± SE. Ca^{2+} sparks, Ca^{2+} waves and F_0 data are obtained from n=25 cells from N= 6 rats for each experimental condition. Caffeine-evoked Ca^{2+} transient data are obtained from n_{CTL}= 9 cells, $n_{CTL+ISO}$= 6 cells, n_{MetS}= 9 cells and $n_{MetS+ISO}$= 9

cells, from N = 3 rats for each experimental condition. *$P \leq 0.05$ respect to the CTL group, † $P \leq 0.05$ respect to the CTL + ISO group and # $P \leq 0.05$ respect to the MetS group.

Table 1.

General characteristics of control and Metabolic Syndrome animals.

	EXPERIMENTAL GROUP	
Parameters	**CTL**	**MetS**
Body Weight (g)	398.1 ± 10.0	524.8 ± 35.0 **
Abdominal Fat (g)	2.7 ± 0.2	11.2 ± 0.8 **
Heart Weight (g)	1.22 ± 0.04	1.28 ± 0.04
HW/BW ratio x 100	0.30 ± 0.01	0.25 ± 0.03 **
LV Weight (g)	0.81 ± 0.02	0.85 ± 0.03
LV/HW ratio	0.67 ± 0.02	0.67 ± 0.02
Tibia Length (cm)	4.2 ± 0.2	4.4 ± 0.4
Triglycerides (mg/dL)	94.3 ± 15.0	269.4 ± 18.0 **
HDL-C (mg/dL)	37.2 ± 2.0	31.7 ± 5.0 *
Glucose (mg/dL)	68.6 ± 6.6	78.5 ± 4.1
TG/HDL-C ratio	2.6 ± 0.4	8.8 ± 0.9 **

Values are mean ± S.E.M of N=11 control rats (CTL), and N=10 metabolic syndrome (MetS) rats. BW, body weight; HDL-C, high-density lipoprotein cholesterol; HW, heart weight; LV, left ventricle; TG, triglycerides.

* $P \leq 0.05$ and

** $P \leq 0.001$ *vs.* CTL animals.

Table 2.

Characteristics of Ca^{2+} spark recorded in control (CTL) and metabolic syndrome (MetS) cardiomyocytes in the absence and presence of Isoproterenol (ISO).

	Experimental condition			
Ca^{2+} spark properties	**CTL**	**CTL+ISO**	**MetS**	**MetS+ISO**
Amplitude (F/F_0)	2.01 ± 0.04	2.11 ± 0.03	2.01 ± 0.03	2.01 ± 0.03
FDHM (ms)	60.3 ± 2.09	52.8 ± 1.34 *	55.7 ± 1.80 *	52.8 ± 1.33 *
FWHM (μm)	3.14 ± 0.05	3.01 ± 0.04	2.92 ± 0.05 *	2.90 ± 0.04 *
RT (ms)	17.6 ± 0.79	17.3 ± 0.66	15.6 ± 0.65	17.2 ± 0.60
TTP (ms)	32.6 ± 2.15	29.2 ± 1.50	27.8 ± 1.53	30.7 ± 1.39
TAU (ms)	90.7 ± 8.55	73.7 ± 5.80	85.6 ± 8.1	71.7 ± 5.88
Spark-mediated Ca^{2+} leak	709.5 ± 52.8	715. 2 ± 38.6	600.2 ±32.9	828.2 ±37.8 **,#

Values are mean ± S.E.M of n=30 cells from N= 6 rats for each experimental condition.

FDHM, full duration at half maximum, FWHM, full width at half maximum; RT, rising time; TTP, time-to-peak; Ca^{2+} leak, calculated as the product of Ca^{2+} spark frequency*Ca^{2+} spark amplitude*FWHM* FDHM. Ca^{2+} spark data are obtained from n_{CTL}= 339 events, $n_{CTL+ISO}$= 471 events, n_{MetS}= 421 events and $n_{MetS+ISO}$= 600 events.

* $P \leq 0.05$ and

** $P \leq 0.001$ *vs.* CTL cells,

\# $P \leq 0.05$ *vs.* MetS cells.

Table 3.

Characteristics of Ca^{2+} spark recorded in control (CTL) and metabolic syndrome (MetS) cardiomyocytes exposed to AIP (10 μM, 1 h); and in the absence or presence of Isoproterenol (ISO).

	Experimental condition			
Ca^{2+} spark properties	**CTL**	**CTL+ISO**	**MetS**	**MetS+ISO**
Amplitude (F/F_0)	2.00 ± .006	2.05 ± 0.05	1.59 ± 0.04 *,†	1.75 ± 0.05 *,†
FDHM (ms)	37.7 ± 1.77	33.4 ± 1.44	39.7 ± 2.01	35.2 ± 1.79
FWHM (μm)	2.71 ± 0.08	2.55 ± 0.07	2.11 ± 0.08 *,†	2.25 ± 0.08 *,†
RT (ms)	17.3 ± 1.14	18.2 ± 01.09	20.6 ± 1.16	20.1 ± 1.30
TTP (ms)	19.7 ± 1.23	18.7 ± 1.08	21.8 ± 1.62 *,†	23.1 ± 2.09 *,†
TAU (ms)	65.2 ± 11.9	96.2 ± 17.1	107 ± 86.9	115 ± 32.2
Spark-mediated Ca^{2+} leak	203.8 ± 19.5	270.7 ± 33.1	144.6 ±16.0 *,†	232.6 ±42.5 *,†

Values are mean ± S.E.M of n=25 cells from N= 5 rats for each experimental condition.

FDHM, full duration at half maximum; FWHM, full width at half maximum; RT, rising time; TTP, time-to-peak; Ca^{2+} leak, calculated as the product of Ca spark frequency*Ca spark amplitude*FWHM* FDHM. Ca^{2+} spark data are obtained from n_{CTL}= 166 events, $n_{CTL+ISO}$= 194 events, n_{MetS}= 165 events and $n_{MetS+ISO}$= 186 events.

$^{*}P \leq 0.05$ vs. CTL cells,

$^{\dagger}P \leq 0.05$ vs. CTL+ISO-treated cells and

$^{\#}P \leq 0.05$ vs. MetS cells.